

## **General Disclaimer**

### **One or more of the Following Statements may affect this Document**

- This document has been reproduced from the best copy furnished by the organizational source. It is being released in the interest of making available as much information as possible.
- This document may contain data, which exceeds the sheet parameters. It was furnished in this condition by the organizational source and is the best copy available.
- This document may contain tone-on-tone or color graphs, charts and/or pictures, which have been reproduced in black and white.
- This document is paginated as submitted by the original source.
- Portions of this document are not fully legible due to the historical nature of some of the material. However, it is the best reproduction available from the original submission.

DEA

FINAL TECHNICAL REPORT FOR NASA GRANT NO. NAG5-47



Introduction

The purpose of this project was to obtain observations of  $\text{Ly}\alpha$  in a set of redshift quasars selected from the Palomar Green survey of bright quasars. The problem that motivated these observations was the well known discrepancies of the hydrogen line strengths in the broad line regions of quasars. The basic plan was to combine ultraviolet, optical, and infrared observations to obtain a data set sampling as broad a range in hydrogen lines as possible in individual quasars. From the measured  $\text{Ly}\alpha$  fluxes, coupled with Balmer and Paschen line fluxes measured in these same objects, it was hoped to establish observational constraints that would guide models of the broad emission line regions of quasars. In addition to this goal, it was found that the IUE spectra were generally of sufficiently high quality to derive line profiles of the ultraviolet lines  $\text{Ly}\alpha$  and CIV 1550Å, which have been compared to the Balmer line profiles. Interesting results have been derived from this comparison.

N84-18122

Unclas  
15240

G3/89

Line Fluxes

The quasars that were observed in this program are listed in Table 1, along with the basic results of the IUE, optical, and infrared observations. The observed fluxes from the ultraviolet, optical, and infrared lines are listed in Table 1 for these quasars. In Table 2, the relative strengths of the emission lines, compared to the nearby continua are listed, as are the relative strengths of the various lines.

The results of Table 2 show that the quasars in this study are far from the simple Case B results, and indeed strain the current model calculations. This is shown in Figure 1, where the Balmer/Paschen line ratios for these quasars are plotted and compared in the other samples of quasars (Soifer, *et al.*, 1981,

(NASA-CR-175376) OBSERVATIONS OF EMISSION  
IN BRIGHT, LOW REDSHIFT QUASARS Final  
Technical Report (California Inst. of Tech.)  
11 p HC A02/EF A01 CSCI 03A

OBSERVATIONS OF QUASAR EMISSION LINES

TABLE 1

Observed Line Fluxes ( $W/m^2$ )

Object	z	$L\alpha$ °	NV °	CIV °	HeII °	H $\alpha$ °	H $\beta$ °	[OIII] °	HeII °	P $\alpha$ °
PG0503+76	0.0987	1216A $\times 10^{-15}$	1240A $\times 10^{-16}$	1550A $\times 10^{-15}$	1670A $\times 10^{-16}$	6562A $\times 10^{-15}$	4861A $\times 10^{-16}$	4959/5007A $\times 10^{-16}$	4861A $\times 10^{-17}$	18750A $\times 10^{-17}$
PG1307+08	0.153	1.8	1.4	1.0	<1.3	0.75	2.0	0.84	<0.5	5.4±1.0
PG1202+28	0.1628	1.7	1.9	1.1	0.2±.1	0.61	1.7		0.8	2.3±0.7
PG1416-12	0.1295	1.3	1.3	1.2	0.9±0.3	1.4	2.3	0.6	<1.4	5.4±1.5
PG1309+35	0.180	0.68	0.9	0.38	0.47	0.62	1.2	1.0	<0.30	3.4±0.9
PG1116+21	0.1723	5.4	8.9	3.3	<11.6	1.5	4.4	4.3	<0.5	9.6±3

NOTE: ALL LIMITS ARE  $3\sigma$

ORIGINAL PAGE IS  
OF POOR QUALITY

Figure 1. The  $P\alpha/H\alpha$  line ratio plotted vs the  $H\alpha/H\beta$  line ratio for quasars and Seyfert galaxies from various samples. The filled circles are Seyfert galaxies, observed by Lacy *et al.* (1982), the open circles are quasars observed by Soifer, *et al.* (1981), and the open squares are quasars observed by Puetter, *et al.* (1981). The open triangles are the quasars observed in this program. The case B line ratios are represented by the point indicated. The case B result viewed through different amounts of reddening, in units of  $E(B-V)$ , is shown by the indicated line. The case  $P\alpha/H\beta = 0.28$  is also shown as a line. The model predictions for these ratios of Krolik and Kwan (1981) are indicated by the lines noted as  $10^{10}$ ,  $4 \times 10^9$ , and  $10^9$ . These indicate electron densities of individual models. The predicted line ratios from the models of Canfield and Puetter (1980) are shown as the line CP.

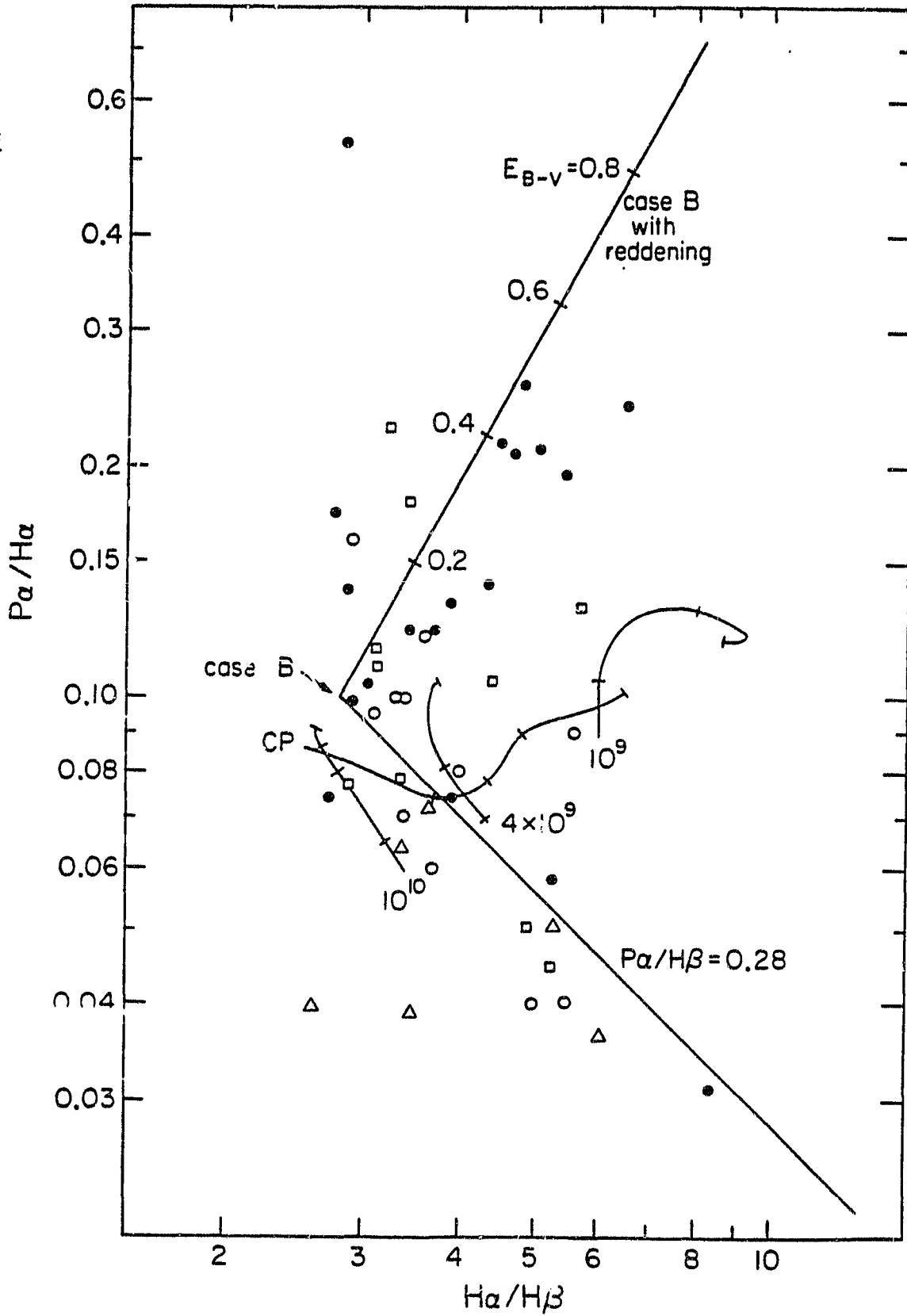


Figure 1

Puetter, *et al.*, 1981) and Seyfert galaxies (Lacy, *et al.*, 1982). In this figure the standard Case B recombination point is indicated, as is the reddened Case B line. Most of the Seyfert galaxies follow this track, strongly suggesting that reddening significantly effects the line ratios in these objects. The quasars in Figure 1 deviate strongly from this line. The quasars in this present study are represented by the open triangles. Most of the quasars show  $P\alpha/H\beta$  ratios close to the recombination, i.e., optically thin ratio of 0.2 - 0.3. Indeed many of these quasars are found to have line ratios quite similar to those predicted by the models of Krolik and Kwan (1981) and those of Canfield and Puetter (1980). Some of the quasars deviate strongly even from these models, most notably two of the quasars from this sample PG 0803+76 and PG 1202+28 show significantly lower  $P\alpha/H\beta$  ratio than can be explained by the quasar emission line models. This discrepancy is hard to understand on physical grounds, since the  $H\beta$  and  $P\alpha$  lines originate in the same level, and the physical mechanisms that have been invoked to decrease the  $L\alpha$  flux compared to the Balmer lines would also likely act to weaken the Balmer lines relative to Paschen  $\alpha$ .

### Line Profiles

Because of the high signal to noise of the  $L\alpha$  and CIV emission lines it was found possible to compare the shape of these lines with the Balmer lines in the brighter quasars to determine if there are systematic differences between the resonance lines represented by  $L\alpha$  and CIV, and the Balmer lines, represented by  $H\beta$  ( $H\beta$  was chosen because of the contamination produced on the  $H\alpha$  profile by the atmospheric B band). Figures 2a, b, and c, show the comparisons of the  $L\alpha$ , CIV, and  $H\beta$  line profiles in 3 quasars from the sample observed by IUE.

From these data it is clear that there are no clear trends in the line shapes, that can be used to guide models of the dynamics of the broad line regions. For

TABLE 2

## RELATIVE EMISSION LINE STRENGTHS

Object	Equivalent Width ( $\text{\AA}$ )						Line Ratio		
	L $\alpha$	NV	CIV	H $\alpha$	H $\beta$	P $\alpha$	L $\alpha$ /H $\beta$	L $\alpha$ /H $\beta$	P $\alpha$ /H $\beta$
PG0803+76	164	8	53	610	130	56	3.5	9.6	0.11 $\pm$ .02
PG1307+08	81	6	75	570	90	125	2.5	9.3	0.27 $\pm$ .05
PG1202+28	323	36	186	955	197	43	2.8	9.9	0.14 $\pm$ .04
PG1416-12	274	30	412	1150	139	159	0.9	5.6	0.23 $\pm$ .06
PG1309+35	91	12	65	502	64	90	1.1	5.7	0.28 $\pm$ .07
PG1116+21	89	15	72	535	92	80	3.6	12.2	0.22 $\pm$ .07

ORIGINAL PAGE IS  
OF POOR QUALITY

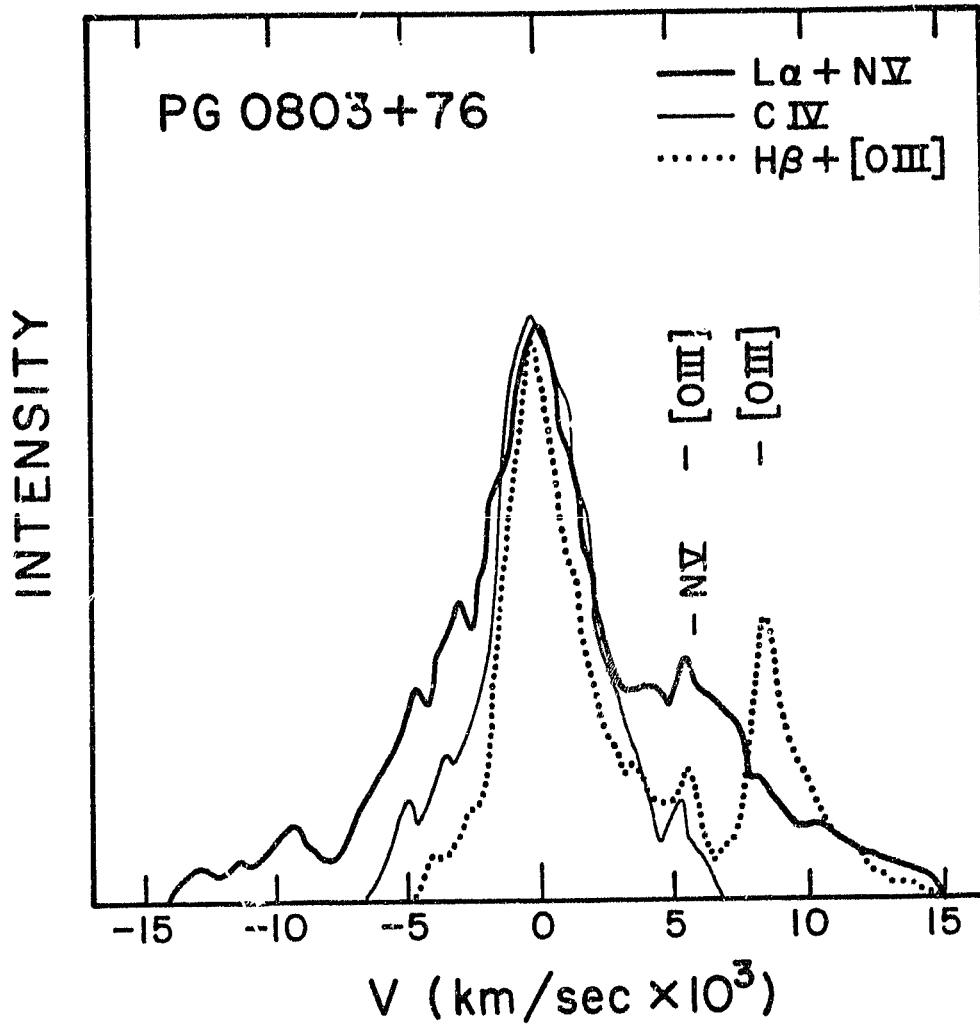
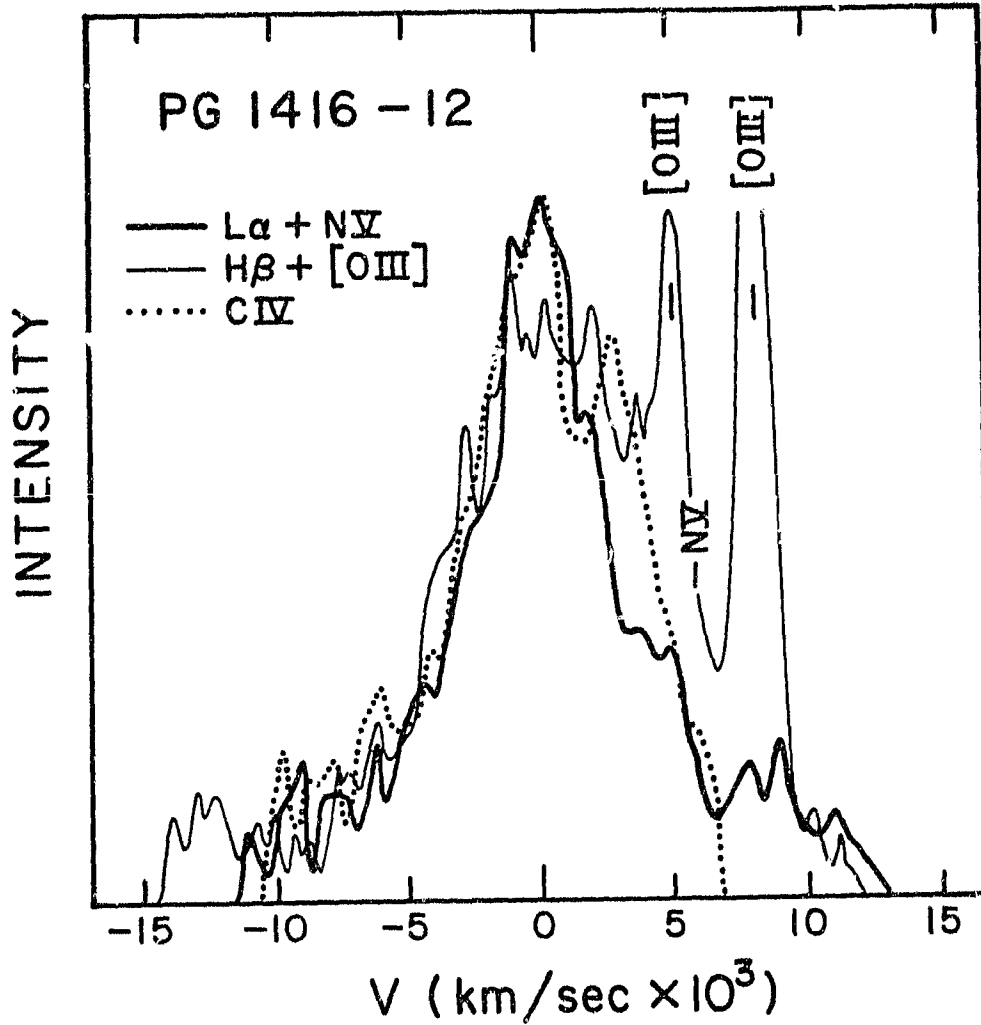


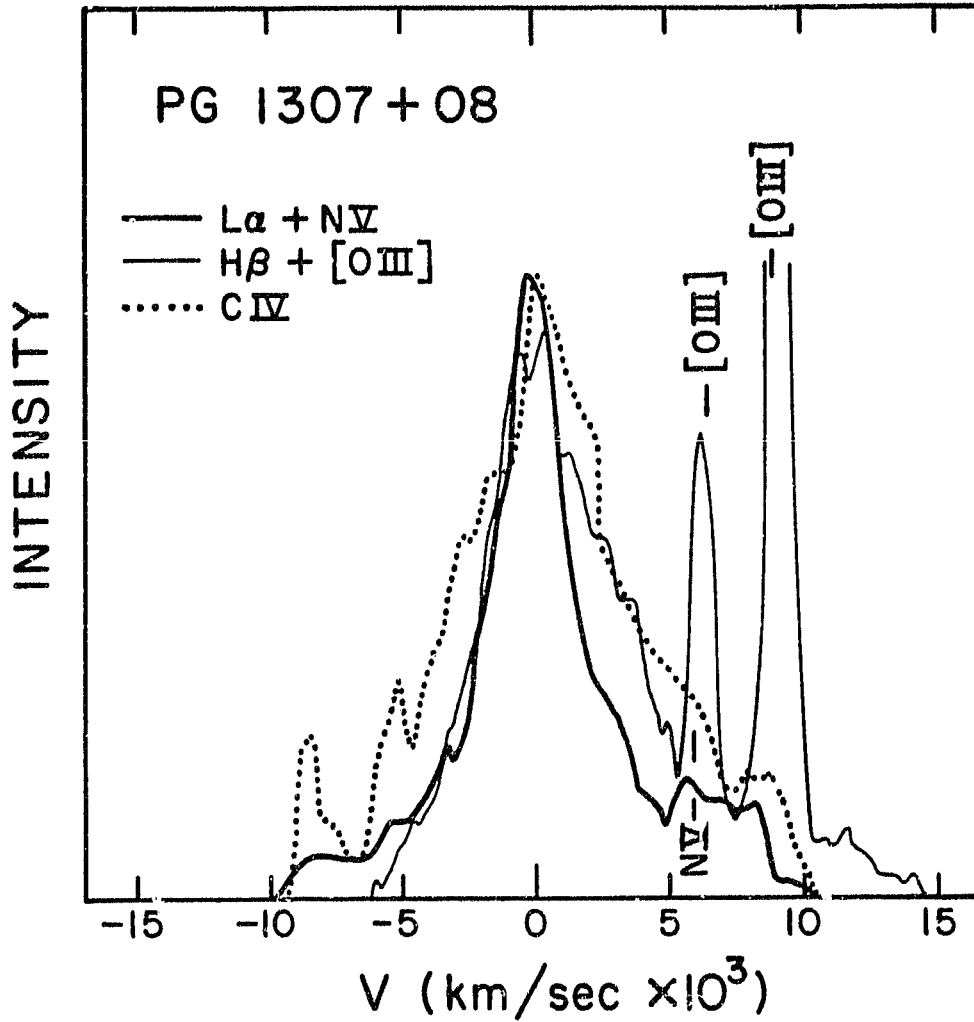
Figure 2a. The line profiles of  $L\alpha$ ,  $C\ IV$  1550  $\text{\AA}$ , and  $H\beta$  plotted as intensity vs velocity with respect to the average redshift for the quasar PG0803+76. No attempt has been made to subtract  $NV$  from the  $L\alpha$  profile, or  $[OIII]$  from the  $H\beta$  profile.

ORIGINAL PAGE 19  
OF POOR QUALITY



2b. The line profiles of  $L\alpha$ ,  $CIV$  1550  $\text{\AA}$ , and  $H\beta$  plotted as intensity vs velocity with respect to the average redshift for the quasar PG1416-12. No attempt has been made to subtract  $NV$  from the  $L\alpha$  profile, or  $[OIII]$  from the  $H\beta$  profile.

ORIGINAL PAGE IS  
OF POOR QUALITY



2c. The line profiles of  $L\alpha$ ,  $CIV$  1550  $\text{\AA}$ , and  $H\beta$  plotted as intensity vs velocity with respect to the average redshift for the quasar P1307+80. No attempt has been made to subtract  $NV$  from the  $L\alpha$  profile, or  $[OIII]$  from the  $H\beta$  profile.

example in PG 0803+76 (Figure 2a)  $\text{L}\alpha$  is broader than CIV (1550Å) which is in turn broader than  $\text{H}\beta$ , while in PG 1416-12 (Figure 2b) the lines are all of roughly equal shape, or if anything, CIV 1550 is broader than the hydrogen lines. The case of PG 1307+08 (Figure 2c) is perhaps the most extreme counter example to the most simple minded models, where  $\text{L}\alpha$  is the narrowest of the permitted lines, with  $\text{H}\beta$  wider, and CIV 1550 widest of all.

### Conclusions

The results described above demonstrate that the search for guiding physical parameters for modeling the quasar broadline regions is most complex, and will not yield readily to observations. The observed hydrogen emission line ratios have shown that the first order models of the broadline regions, such as those developed by Canfield and Puetter (1981) and Kwan, Krolik (1981) fit the data adequately but not well enough to claim clear understanding. In particular the examples of extremely weak  $\text{P}\alpha$  lines in two quasars are quite difficult to understand based on current models of the broad line regions.

In addition, the line profiles shown in Figure 2 cause significant difficulties with many of the dynamic models of the permitted line emitting gas, since such models predict systematic trends in line shape with line optical depth, as displayed by the  $\text{L}\alpha$ , CIV, and  $\text{H}\beta$  lines, whereas the observed profiles show no such trends.

## REFERENCES

Canfield, R. C. and Puetter, R. C. 1980, *Ap. J. (Letters)*, **236**, L7.

Kwan, J. and Krolik, J. H. 1981, **250**, 478.

Lacy, J. H., *et al.*, 1982, *Ap. J.*, **256**, 75.

Puetter, R. C., Smith, H. E., Willner, S. P., and Pipher, J. L. 1981, *Ap. J.*, **243**, 345.

Soifer, B. T., Neugebauer, G., Oke, J. B., and Matthews, K. 1981, *Ap. J.*, **243**, 389.